

Temperature dependence of the excitonic band gap in $\text{In}_x\text{Ga}_{1-x}\text{As}/\text{GaAs}$ self-assembled quantum dots

G. Ortner,* M. Schwab, and M. Bayer

Experimentelle Physik II, Universität Dortmund, D-44221 Dortmund, Germany

R. Pässler

Technische Universität Chemnitz, Institut für Physik, D-09107 Chemnitz, Germany

S. Fafard, Z. Wasilewski, and P. Hawrylak

Institute for Microstructural Sciences, National Research Council, Ottawa, K1A 0R6, Canada

A. Forchel

Technische Physik, Universität Würzburg, Am Hubland, D-97074 Würzburg, Germany

(Received 19 December 2003; revised manuscript received 31 January 2005; published 15 August 2005)

Single-dot spectroscopy was used to determine the temperature dependence of the ground-state exciton energy $E(T)$ in self-assembled $\text{In}_x\text{Ga}_{1-x}\text{As}/\text{GaAs}$ quantum dots (QDs) from $T=2$ up to ~ 100 K. Differences of dot composition and geometry are manifested primarily in the absolute transition energies, whereas the band-gap reduction depends only weakly on microscopic details. $E(T)$ can be well described by semiempirical phonon-dispersion models developed recently for bulk, suggesting that thermal lattice expansion and electron-phonon interaction are the dominant mechanisms for $E(T)$, whereas QD-specific mechanisms seem to be of minor importance, in contrast to observations for nanocrystals.

DOI: [10.1103/PhysRevB.72.085328](https://doi.org/10.1103/PhysRevB.72.085328)

PACS number(s): 71.35.Ji, 71.70.Ej

I. INTRODUCTION

During the last decade, spectroscopy of single quantum dots (QDs) has become a central research activity of semiconductor physics [see e.g., Refs. 1 and 2]. This interest arises from the three-dimensional (3D) confinement of carriers in them, because of which they often are termed “artificial atoms”. This nomenclature has been supported by the observation of spectrally sharp exciton emission with reported linewidths down in the few microelectron-volt range at cryogenic temperatures.^{3–5} However, although for atoms the coupling to the environment is mostly small, for QDs the embodiment into a crystal matrix cannot be neglected, as recent studies of exciton dephasing demonstrate; above ~ 50 K the spectral linewidth broadens rather strongly becoming similar to the widths observed for structures of higher dimensionality. Furthermore, underneath this line a broad background appears due to phonon-assisted transitions.⁶

Because of the high precision of single-dot spectroscopy it might be possible to address basic problems of semiconductor physics with unprecedented accuracy. One of these basic problems is the temperature dependence of the band gap $E(T)$. As origin for the reduction of the gap two mechanisms have been identified for bulk systems: scattering of electrons by phonons and thermal expansion of the lattice. Various simple models have been used for numerical simulations of bulk $E(T)$.^{7–10} Most widely known is Varshni’s formula,⁷ which represents a combination of a quadratic low-temperature asymptote with a linear high-temperature dependence.

Following this model, in most experimental studies a decrease proportional to T^2 has been assumed for $E(T)$ at cryo-

genic temperatures. Because of the often rather broad spectral lines, due to either limited crystal quality or intrinsic homogeneous broadening, the available data appeared to be in agreement with this model. However, recently Cardona *et al.* could demonstrate strong deviations from a quadratic dependence by performing resonant Raman scattering with microelectron-volt resolution on bulk Si, revealing a band-gap reduction proportional to T^4 below 4 K.¹¹

The interest in semiconductor nanostructures raises questions about $E(T)$ in these systems. For the vast majority of them, with increasing temperature a monotonous decrease of the gap has been observed, which is similar to the bulk behavior. In many cases, in particular also for QDs, the data could be reasonably well described by a T^2 dependence within the experimental accuracy, irrespective of the restricted validity of the Varshni model. Here, single-dot spectroscopy might allow for more accurate insight into the dependence of $E(T)$ as well as its origin.

No detailed theory, either first principles or semiempirical, that would allow for an accurate description of $E(T)$, seems to be available for QDs. The two aforementioned bulk mechanisms certainly will also contribute to $E(T)$ in dots, but significant changes are expected for them: (a) depending on the QD environment the thermal lattice expansion could vary considerably from the bulk reference. (b) Three-dimensional carrier confinement changes both the electronic and phononic level structure and thus the electron-phonon interaction should be strongly modified. To give just one example of an expected change: it has been found that a weak-coupling model treating the interaction of electrons and phonons perturbatively (as it is used in GaAs-based structures of higher dimensionality) is no longer adequate, but

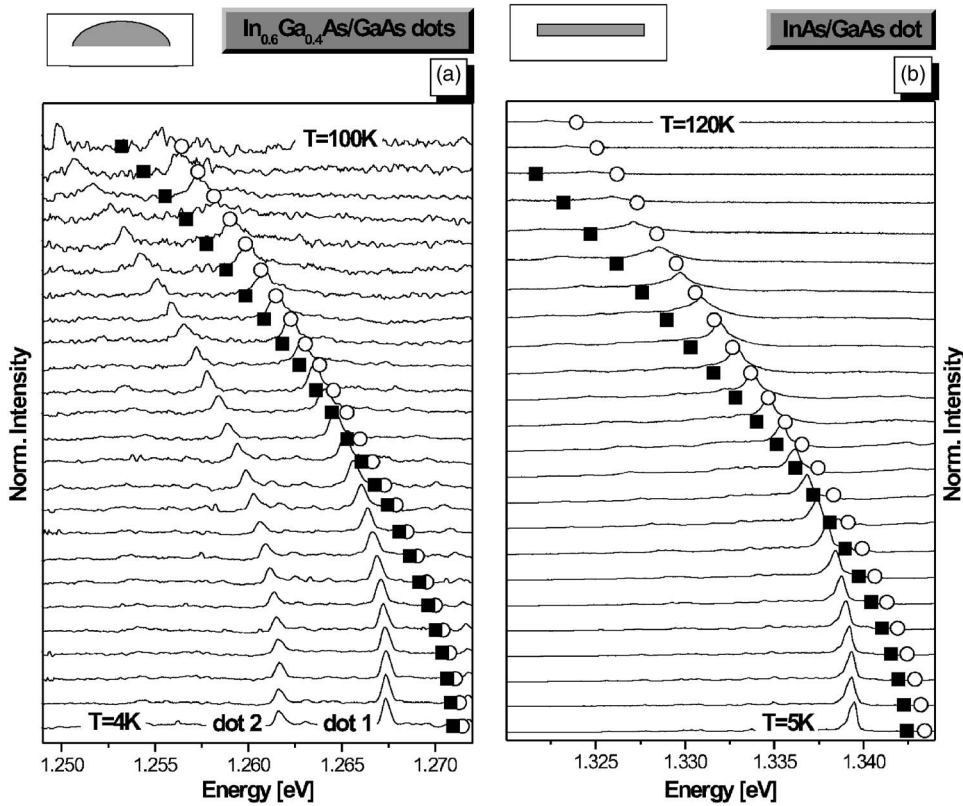


FIG. 1. Photoluminescence spectra of (a) two $\text{In}_{0.60}\text{Ga}_{0.40}\text{As}/\text{GaAs}$ QDs for temperatures from $T=4$ up to 100 K (in steps of 4 K) and (b) an InAs/GaAs QD from $T=5$ up to 120 K (in steps of 5 K). The excitation power was 0.3 mW in each case. The sketches schematically show the geometries of the two dot types. The symbols in each panel give the energy shift of bulk GaAs (the solid symbols) and InAs (the open symbols).

strong, polaronlike coupling has to be assumed in dot structures.^{12,13}

In addition, different mechanisms for $E(T)$ might become important for QDs, as demonstrated by experimental studies on nanocrystals; because of the confinement of the wave function in them, the excitonic energy gap increases with decreasing nanocrystal size d . In some cases it has been found that the $E(d)$ dependencies vary with lattice temperature T , implying a dependence of the temperature-induced band-gap shift $E(T)$ on nanocrystal diameter.^{14,15} The $E(T)$ are approaching the limiting asymptote of bulk only when d becomes larger than or at least comparable to the exciton Bohr radius a_B (representing the so-called large-cluster limit). An example for such a mechanism is the increase of the confined wave function spread by the temperature-induced lattice expansion, because of which the confinement energy is reduced.

The main goal of the present paper is to show that unlike for nanocrystals, the origin for the $E(T)$ dependence in self-assembled $\text{In}_{1-x}\text{Ga}_x\text{As}/\text{GaAs}$ QDs lies dominantly in the same mechanisms as for bulk, whereas dot-specific influences apparently are small. Phonon-dispersion models developed for bulk, such as a higher-order root representation¹⁶ or a two-oscillator model,¹⁷ describe the band-gap reduction $E(T)$ by temperature very well. This extrapolation of analytical models to QDs is possible even though the exciton Bohr radius a_B is quite a bit larger than the dot size d (“small-cluster limit”).

Precise information on the $E(T)$ dependencies in QDs are of great interest, as low-temperature variations have been suggested as the “control knob” in quantum devices: an instance is a single-photon emitter that produces photons on

demand and is necessary for technical implementations of quantum information technology, such as quantum cryptography.¹⁸ Such a device might be realized by a single QD located in a resonator. The spontaneous emission from this dot can be controlled by varying the energy of its ground-state exciton transition relative to a confined optical resonator mode. One possibility for such a variation is changing the temperature,¹⁹ besides others like application of DC electric field, AC-Stark effect, etc.

II. EXPERIMENT

In this work we have studied two different types of self-assembled QDs fabricated by MBE. The first type was the QDs with a material composition $\text{In}_{0.60}\text{Ga}_{0.40}\text{As}$ in the dot and GaAs in the barrier. From scanning electron microscopy of a sample, in which the QDs were not covered by a cap layer, their geometry is approximately lens shaped, with a diameter $d \approx 20$ nm and height $h \approx 6$ nm. The second type of QDs was the InAs/GaAs structures, where the self-assembled growth had been extended by an indium flush²⁰ resulting in disk like QDs with diameter $d \approx 20$ nm and height $h \approx 2$ nm. Thus the two dot types differ significantly in composition and geometry, as sketched in Fig. 1. The energy of the ground-state exciton emission of the $\text{In}_{0.60}\text{Ga}_{0.40}\text{As}/\text{GaAs}$ QDs is located in a range from 1.25 to 1.30 eV, and that of the InAs/GaAs dots ranges from 1.31 to 1.36 eV.

One remark should be made on the QD material composition: it has been shown by high resolution microscopy that during growth an intermixing²¹ of Ga and In occurs, smoothing the confinement potential and reducing its depth.^{22,23}

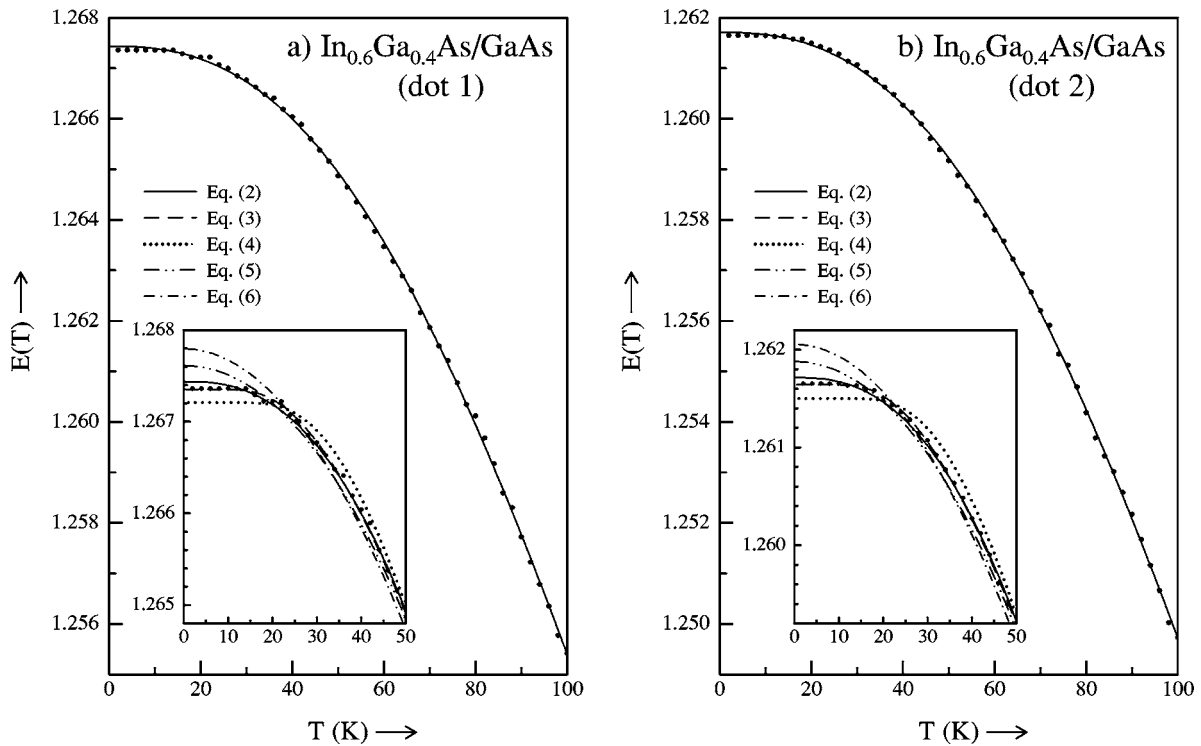


FIG. 2. $E(T)$ curves obtained by least-mean-square fits of the experimental data for the $\text{In}_{0.6}\text{Ga}_{0.4}\text{As}/\text{GaAs}$ dots 1 and 2 of Fig. 1(a). The insets show the low-temperature sections of the fit curves resulting from the power-function model Eq. (2), the two-oscillator model Eq. (3), the Bose-Einstein model Eq. (4), Varshni's model Eq. (5), and the quadratic approximation of the latter Eq. (6).

Since detailed information on deviations from the nominal compositions is not available, we will still refer to the structures as InAs/GaAs and $\text{In}_{0.6}\text{Ga}_{0.4}\text{As}/\text{GaAs}$ QDs, respectively.

For single-dot spectroscopy both samples were patterned, providing mesa structures with lateral sizes down to ~ 100 nm. The samples were mounted either in a He-flow or a He-bath cryostat, allowing us to reduce the sample temperature down to $T=2$ K. To obtain a sufficiently high accuracy for temperature-related shifts, T was varied in steps of 2 K below 40 K and in steps of 4 or 5 K above. We used a frequency-doubled Nd-YAG laser for non-resonant optical excitation with low power densities so that only single electron-hole recombination is monitored. The emission was dispersed by a monochromator ($f=0.5$ m, 600 lines/mm) and detected by a liquid-nitrogen-cooled Si CCD camera providing a spectral resolution of ~ 50 μeV in this configuration.

Photoluminescence spectra of two $\text{In}_{0.6}\text{Ga}_{0.4}\text{As}/\text{GaAs}$ QDs for T from 2 up to 100 K are shown in Fig. 1(a) and the resulting temperature dependencies of the emission energies $E(T)$ are shown by the full circles in Figs. 2(a) and 2(b). Both lines shift monotonically to lower energies with increasing temperature. Similar observations are made for the single InAs/GaAs QD, for which the photoluminescence spectra from $T=2$ up to 120 K are shown in Fig. 1(b) and the corresponding data for $E(T)$ are given in Fig. 3. For both dot types, the emission lines broaden considerably with increasing temperature. In particular, broad sidebands due to phonon-assisted transitions are observed for temperatures above 50 K, as discussed in Refs. 24 and 25.

Here we used nonresonant excitation into the GaAs barriers for optimizing the signal strength, resulting in significantly larger spectral linewidths than would be expected from the radiative exciton decay time. The origin of this broadening is a fluctuating charge environment around the dot, which leads to a spectral diffusion of the emission line during the time used for recording a spectrum (in our case 120 s).²⁶ The charge-induced Stark shifts occur symmetrically around the genuine exciton energy.^{27,28} Therefore, the accuracy of the determination of the QD emission energy is only marginally reduced for these experimental conditions. This is supported by studies with below band-gap excitation conditions, but reduced temperature resolution. In these studies basically the same data for $E(T)$ were obtained as for above-gap excitation.³

III. DISCUSSION OF EXPERIMENTAL DATA

Let us first compare the temperature dependencies of the exciton emission energies in the two QD types to the behaviors in the related bulk materials GaAs²⁹ and InAs.³⁰ These shifts are indicated in Fig. 1 by the solid symbols for GaAs and the open symbols for InAs, where we have shifted the $T=0$ energies of the bulk band gaps to appear in the range of the corresponding dot emission. The shift of the QD gaps is weaker than the shifts in the 3D crystal at very low temperatures, where almost no T dependence at all is observed. This might be expected if one refers to the $E(T)$ mechanisms for bulk: at low temperatures only long-wavelength phonons are excited, for which the electron-phonon interaction is very

much reduced in an object smaller than the wavelength of the lattice vibration, as is the case of a quantum dot. However for higher temperatures, above 50 K, the bulk and QD gaps to a good approximation shift in parallel to lower energies as seen in Fig. 1(a). This is the T range where for example exciton dephasing studies in self-assembled dots have shown that the interaction strength of phonons with confined carriers becomes strong and leads to linewidths similar to those for higher-dimensional systems.⁶

Now let us turn to the comparison of the $E(T)$ in the $\text{In}_{0.60}\text{Ga}_{0.40}\text{As}/\text{GaAs}$ and InAs/GaAs dots in Figs. 2 and 3. Experimentally we find only very small differences for the $E(T)$ between these dots, despite of the significant differences in dot composition and geometry. The low- T plateau is a bit more extended for the $\text{In}_x\text{Ga}_{1-x}\text{As}$ dots as compared to the InAs dots. Neglecting these tiny differences that might hint at dot-inherent origins of $E(T)$, this suggests that any QD-specific origins do not seem to be of major relevance for the band-gap reduction, as they should manifest themselves in distinct differences between the two dot types. On the contrary, the behavior appears to be dominated by the same mechanisms as in bulk, a combination of electron-phonon interaction and thermal lattice expansion. Before we discuss this finding in more detail, we want to compare our data to that reported in literature for other $\text{In}_x\text{Ga}_{1-x}\text{As}/\text{Al}_y\text{Ga}_{1-y}\text{As}$ self-assembled dot systems.

Although in most of these types of investigations the magnitude of the temperature-induced shifts was not the center of interest, but the variation of T served as tool for inducing state resonances, studying electron-phonon interaction, etc.,^{19,24,25,31} these investigations inherently also give infor-

mation about $E(T)$. The comparison shows that within the experimental accuracy the reported shifts are basically identical to the ones observed here, although the dot systems have strong variations in shape, size, composition, strain, etc. This strongly supports our conclusion that dot-inherent properties are not dominant for $E(T)$.

Let us now list the QD-specific mechanisms, which have been addressed in detail in a recent work¹⁵ on PbS nanocrystals: (i) the temperature dependence of the strain from whose release the energies of the confined valence band levels, e.g., in self-assembled QDs might be strongly reduced. (ii) the temperature dependence of the band gap due to the confinement energy reduction that is caused by the lattice expansion and the resulting expansion of the envelope wave function.

The importance of these mechanisms depends on the dot size: in qualitative agreement with calculations for the PbS nanocrystals it was demonstrated, that the two bulk mechanisms are dominating over the QD-specific ones, as long as the QD size is much larger than the exciton Bohr radius a_B . It also holds to a good approximation down to sizes comparable to a_B , but fails for smaller sizes. It is exactly this latter regime that we address with self-assembled QDs, which are generally considered as dot structures in the strong coupling regime. Therefore dot-related mechanisms are expected to become important, and bulk models for $E(T)$ are supposed to fail, in contrast to the experimental findings. Although one might argue that the lateral dot sizes are not that much different from the exciton Bohr radii, their heights are, in any case, much smaller.

However, previous investigations have shown that many electronic phenomena involving phonons in these dots can often be satisfactorily treated by considering the interaction of confined carriers with a bulk phonon bath (see, for example, Refs. 12 and 32). Although we cannot give an ultimate reason for the rather small influence of dot-specific influences, as this would require detailed theoretical modeling, we want to give at least a qualitative argumentation.

For self-assembled QDs the lattice expansion should not differ too much from the homogeneous semiconductors that form the heterostructures. As compared to nanocrystals with a radius of only a few nanometers, the volume of the self-assembled dot structures is still quite a bit larger so that the relative temperature-induced changes are, in effect, considerably smaller. For example, the change of the envelope wavefunction extension affects mostly the confinement energy along the heterostructure growth direction, whereas the effects on the lateral confinement are comparatively weak, in contrast to the 3D changes in the nanocrystals.

Turning to the strain modification, here most probably also the embodiment of the nanocrystals in a glass matrix¹⁵ has to be regarded, which, from a crystallographic point of view, is an environment very much different from that of a self-assembled dot. Dot system and surrounding are much more comparable for these QD systems; they have the same crystal structure except for a lattice mismatch of maximum 7%. In summary, this might lead to the dominance of the mechanisms that are important for the band-gap reduction in bulk also for self-assembled $\text{In}_x\text{Ga}_{1-x}\text{As}/\text{GaAs}$ quantum dots.

The small differences between the $E(T)$ of the two QD types, however, might result from dot-specific origins: for

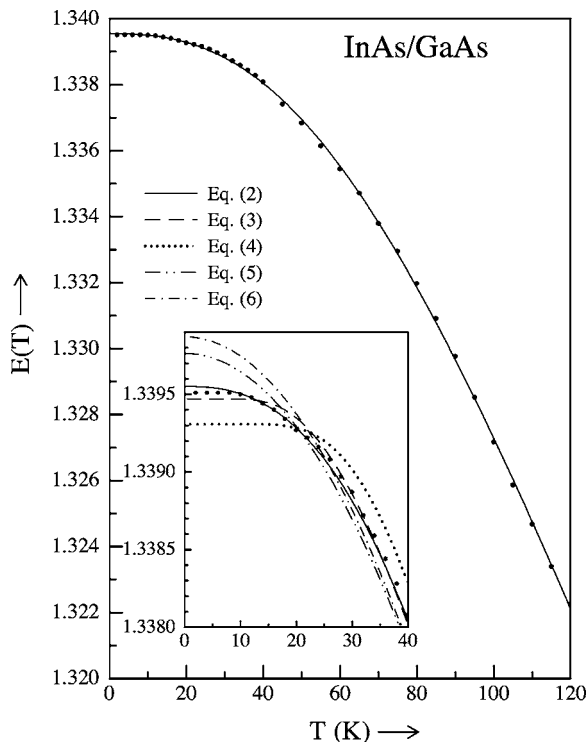


FIG. 3. Same as Fig. 2, but for the single InAs/GaAs QD of Fig. 1(b).

TABLE I. Parameter sets obtained by least-mean-square fits of the $E(T)$ data sets of Figs. 2(a), 2(b), and 3 by the power-function model [Eq. (2)] and the two-oscillator model [Eq. (3)]. The relative errors of the fit parameters are below 5%.

QD system	Eq.	$E(0)$ (meV)	α (meV/K)	ν	ε_c (meV)	Θ (K)	Δ	$W_1=1-W_2$	Θ_1 (K)
In _{0.6} Ga _{0.4} As/GaAs (dot 1)	(2)	1267.43	0.356	1.53	30	208	0.43		
	(3)	1267.35	0.405			240	0.43	0.34	95
In _{0.6} Ga _{0.4} As/GaAs (dot 2)	(2)	1261.71	0.355	1.52	30	209	0.43		
	(3)	1261.64	0.406			241	0.43	0.33	94
InAs/GaAs	(2)	1339.55	0.348	1.51	29	200	0.44		
	(3)	1339.46	0.387			232	0.46	0.38	95

the In_{0.60}Ga_{0.40}As dots, the low- T plateaus are a bit more extended than for the InAs dots, for which we expect a stronger strain field, so that a temperature increase may affect these structures more than the In_{0.60}Ga_{0.40}As dots. In addition, the height of the InAs is only ~ 2 nm, which is 2–3 times smaller than that of the In_{0.60}Ga_{0.40}As dots. Thus a thermal lattice expansion will lead to a considerably stronger reduction of the confinement energy along the heterostructure growth direction in the InAs dots.

IV. ANALYTICAL MODELS FOR $E(T)$

Following the discussion above, it is appropriate to check whether models developed for bulk may be used for describing $E(T)$ in the dot structures. For both mechanisms that have to be considered then, the electron-phonon interaction and the thermal lattice expansion, the contributions of the individual lattice oscillators with energies $\varepsilon = \hbar\omega$ are proportional to the average phonon occupation number $\bar{n} = [\exp(\varepsilon/k_B T) - 1]^{-1}$.^{10,33} $E(T)$ can therefore be represented as

$$E(T) = E(0) - \frac{\alpha}{k_B} \int d\varepsilon \frac{\varepsilon w(\varepsilon)}{\exp(\varepsilon/k_B T) - 1}. \quad (1)$$

Here $\alpha = -dE(T)/dT|_{T \rightarrow \infty}$ is the slope of the linear T dependence in the high temperature limit, and $w(\varepsilon) \geq 0$ is the normalized weighting function of the phonon oscillators, $\int d\varepsilon w(\varepsilon) = 1$. Different assumptions for $w(\varepsilon)$ lead to the several models discussed in the following.

A convenient analytical treatment of $E(T)$ is obtained by a power-function ansatz:¹⁶ $w(\varepsilon) = \nu(\varepsilon/\varepsilon_c)^{\nu-1}/\varepsilon_c$, $\nu > 0$ for ε up to the cutoff energy ε_c of the phonon spectrum, and $w(\varepsilon) = 0$ above. In this model, the $T \rightarrow 0$ asymptotes are given by power functions $[E(0) - E(T)] \propto T^p$, where the fractional exponent p usually ranges from 2 to 3.^{34,35} A detailed analysis shows that for the frequently observed regime of intermediate to large phonon dispersion $E(T)$ is¹⁶

$$E(T) = E(0) - \frac{\alpha\Theta}{2} \left\{ \left[1 + \sum_{n=1}^3 a_n(\nu) \left(\frac{2T}{\Theta} \right)^{n+\nu} + \left(\frac{2T}{\Theta} \right)^{5+\nu} \right]^{1/(5+\nu)} - 1 \right\}, \quad (2)$$

with the expansion coefficients $a_n(\nu)$

$$a_1(\nu) = \frac{5 + \nu}{6} \left(\frac{\pi}{2} \right)^{2+(\nu-1)^2/2},$$

$$a_2(\nu) = \frac{1 - \nu}{2},$$

$$a_3(\nu) = \frac{(5 + \nu)(1 + \nu)^2}{3\nu(2 + \nu)}.$$

The average phonon temperature³³ $\Theta = \langle \varepsilon \rangle / k_B = \nu \varepsilon_c / [k_B(1 + \nu)]$, leading to a cutoff energy $\varepsilon_c = k_B \Theta (1 + \nu) / \nu$. The dispersion coefficient³³ $\Delta = \sqrt{\langle \varepsilon^2 \rangle - \langle \varepsilon \rangle^2} / \langle \varepsilon \rangle$ is $1 / \sqrt{\nu(2 + \nu)}$.¹⁶ Besides the zero-temperature energy, this model contains three parameters for fitting the experimental data.

As an alternate to the power-function model, let us consider a two-oscillator model.¹⁷ For it, the weighting function is given by $w(\varepsilon) = W_1 \delta(\varepsilon - \varepsilon_1) + W_2 \delta(\varepsilon - \varepsilon_2)$, where $\varepsilon_{1,2}$ are the energies of the oscillators with weights $W_{1,2}$. $E(T)$ is then

$$E(T) = E(0) - \alpha \left(\frac{W_1 \Theta_1}{\exp(\Theta_1/T) - 1} + \frac{(1 - W_1) \Theta_2}{\exp(\Theta_2/T) - 1} \right), \quad (3)$$

with phonon temperatures $\Theta_{1,2} = \varepsilon_{1,2} / k_B$. The average phonon temperature and the dispersion coefficient are $\Theta = W_1 \Theta_1 + (1 - W_1) \Theta_2$ and $\Delta = \sqrt{(\Theta_2 - \Theta)(\Theta - \Theta_1)} / \Theta$, respectively.¹⁷ The number of fit parameters is increased to 4, plus the zero- T emission energy. The high-energy oscillator comprises the effects of LA, LO, and TO phonons, the energies of which are a factor of ~ 3 larger than those of the short-wavelength TA phonons forming the low-energy oscillator. This oscillator, therefore, dominates in the cryogenic region. The effective phonon temperature Θ_2 of the high-energy oscillator can be reasonably determined only from data also covering temperatures significantly higher than 100 K. Here we have chosen $\Theta_2 = 315$ K, the same value as for bulk GaAs. The remaining parameters of the model have been determined by fits and are given in Table I, together with the fit parameters obtained from Eq. (2). The relative errors of the fit parameters are below 5%.

Let us now address the comparison of the two models with the experimental data: despite of the differences between confinement potentials, we find almost equal values of the parameters α and Θ for the In_{0.60}Ga_{0.40}As and the InAs dots, independent of the model Eqs. (2) or (3). This under-

TABLE II. Parameter sets of the fits to the experimental data according to the Bose-Einstein model Eq. (4), the Varshni formula Eq. (5), and the limiting two-parameter version of the latter Eq. (6). The relative errors of the fit parameters are below 5%.

QD system	Eq.	$E(T=0)$ (meV)	$\alpha_{B/V}$ (meV/K)	Θ_B, β (K)	$\alpha_V/\beta, c$ (meV/K ²)	$k_B\Theta_B$ (meV)
In _{0.6} Ga _{0.4} As/GaAs dot 1	(4)	1267.22	0.260	144	-	12.4
	(5)	1267.59	-0.484	-490	$0.99 \cdot 10^{-3}$	-
	(6)	1267.77	($\rightarrow\infty$)	($\rightarrow\infty$)	$1.22 \cdot 10^{-3}$	-
In _{0.6} Ga _{0.4} As/GaAs (dot 2)	(4)	1261.50	0.259	144	-	12.4
	(5)	1261.88	-0.495	-501	$0.99 \cdot 10^{-3}$	-
	(6)	1262.05	($\rightarrow\infty$)	($\rightarrow\infty$)	$1.22 \cdot 10^{-3}$	-
InAs/GaAs	(4)	1339.33	0.280	149	-	12.8
	(5)	1339.76	-2.233	-1912	$1.17 \cdot 10^{-3}$	-
	(6)	1339.82	($\rightarrow\infty$)	($\rightarrow\infty$)	$1.24 \cdot 10^{-3}$	-

lines that the primary consequence of varying the QD system is a different absolute energy position, whereas the temperature-induced shift $E(T)$ relative to the $E(T=0)$ energy is only weakly affected by changes of geometry and composition.

In the two-oscillator model, the estimation of $\Theta_1=95$ K for the phonon temperature of the low-energy oscillator in both QD systems corresponds to a phonon energy of $k_B\Theta_1=8.2$ meV. This energy is located just between the two closely spaced bulk GaAs TA phonon peaks, $\hbar\omega_{TA}(L)=7.7$ meV and $\hbar\omega_{TA}(X)=9.8$ meV in the phonon density of states.³⁶ This indicates that the $E(T)$ dependencies of QDs are determined mainly by the interaction of the electronic systems with phonons of the host material.

The temperature dependence of $E(T)$ at low T for the In_{0.60}Ga_{0.40}As/GaAs dots is somewhat weaker than expected from the power function model: here the two-oscillator model provides a better fit because the measured energies are constant from 2 up to almost 15 K. On the other hand, for the InAs/GaAs QDs, the power-function model gives a slightly better fit to the data throughout the whole temperature range. Yet, in view of the small differences (<0.1 meV) from experiment and among each other, both models can generally be considered as good approaches for numerical simulations of $E(T)$ dependencies in QDs.

In a large number of studies concerning the temperature dependencies of energy gaps in semiconductors, Varshni's formula^{7,8} or expressions of Bose-Einstein type^{9,10} have been used for fitting $E(T)$ data sets. In these models it is not possible to adjust the system-specific degree of phonon dispersion (quantified by the dispersion coefficient Δ). Instead, both models involve fixed Δ values.^{16,37} On the other hand, the numerical effort for data fits is considerably smaller, so it is worth also testing their applicability to describing QD data with high accuracy.

Let us consider first the Bose-Einstein model, which describes the limiting case of completely vanishing dispersion $\Delta=0$. For direct comparison of the model parameters with those from the phonon-dispersion models it can be rewritten in the form^{35,37,38}

$$E_B(T) = E_B(0) - \frac{\alpha_B \Theta_B}{\exp\left(\frac{\Theta_B}{T}\right) - 1} \\ = E_B(0) - \frac{\alpha_B \Theta_B}{2} \left[\coth\left(\frac{\Theta_B}{2T}\right) - 1 \right], \quad (4)$$

where $\Theta_B = \varepsilon_B/k_B$ is the temperature of the phonon oscillator, giving a total of three fit parameters (listed for the two dot types in Table II). The fitted dependencies are shown by the dotted curves in the insets to Figs. 2(a), 2(b), and 3. In comparison to the two-oscillator model, the Bose-Einstein model curves show more extended and energetically lowered plateaus.

$$E_V(T) = E_V(0) - \frac{\alpha_V T^2}{\beta + T} \quad (5)$$

is the Varshni model with three fit parameters as well.^{7,8} Here β is expected to be comparable with the Debye temperature. When fitting the experimental data sets by Eq. (5), however, one is facing a factually unlimited (order-of-magnitude) floating of the parameters $\alpha_V > 0$ and $\beta > 0$ toward infinity.^{16,34} Such a limiting transition corresponds to $E_V(T)$ approaching a quadratic dependence^{34,37,38}

$$E_V(T) \rightarrow E_Q(T) = E_Q(0) - c_V \cdot T^2, \quad (6)$$

where $c_V = \lim_{\beta \rightarrow \infty} (\alpha_V/\beta)$. From computational points of view, Eq. (6) has the advantage that it comprises only two parameters: the $T=0$ energy and the curvature parameter c_V (see Table II). The corresponding parabolas are shown by the dashed-dotted curves in Figs. 2 and 3. For $T < 20$ K, the descent of these curves is much stronger than those of the experimental data.

From a formal point of view, it is possible to achieve a reduction of the curvature of $E_V(T)$ by admitting negative values, $\alpha_V < 0$ and $\beta < 0$, in Varshni's model. The corresponding values are also listed in Table II. Yet, from the dashed-double-dotted curves in Figs. 2 and 3, we see that even then no good simulation of the behavior can be obtained. Moreover, negative parameter values obviously represent a situation of no physical relevance. In summary the

simple models Eqs. (4)–(6) cannot give reasonable descriptions of experimental data for $E(T)$.

V. SUMMARY

The temperature-dependent energy shifts of the exciton emission in different $\text{In}_x\text{Ga}_{1-x}\text{As}/\text{GaAs}$ QD samples at cryogenic temperatures can be well described by the power function and the two-oscillator model, developed recently for bulk materials. QD-specific mechanisms are apparently small

for self-assembled dots: structural variations such as different compositions and geometries have only little influence on the temperature dependencies, which are mostly determined by coupling to the bulk phonon system of the material in which the QDs are embedded.

ACKNOWLEDGMENT

The authors would like to thank the Deutsche Forschungsgemeinschaft for financial support of the experimental part of this work.

*Electronic address: gerhard.ortner@physik.uni-dortmund.de

- ¹A. Zrenner, J. Chem. Phys. **112**, 7790 (2000).
- ²D. Gammon and D. G. Steel, Phys. Today **55** (10), 36 (2002).
- ³M. Bayer and A. Forchel, Phys. Rev. B **65**, 041308(R) (2002).
- ⁴C. Kammerer, C. Voisin, G. Cassabois, C. Delalande, Ph. Roussignol, F. Klopff, J. P. Reithmaier, A. Forchel, and J. M. Gérard, Phys. Rev. B **66**, 041306(R) (2002).
- ⁵K. Leosson, D. Birkedal, I. Magnúsdóttir, W. Langbein, and J. M. Hvam, Physica E (Amsterdam) **17**, 1 (2003).
- ⁶P. Borri, W. Langbein, S. Schneider, U. Woggon, R. L. Sellin, D. Ouyang, and D. Bimberg, Phys. Rev. Lett. **87**, 157401 (2001).
- ⁷Y. P. Varshni, Physica (Utrecht) **34**, 149 (1967).
- ⁸C. D. Thurmond, J. Electrochem. Soc. **122**, 1133 (1975).
- ⁹L. Vina, S. Logothetidis, and M. Cardona, Phys. Rev. B **30**, 1979 (1984).
- ¹⁰K. P. O'Donnell and X. Chen, Appl. Phys. Lett. **58**, 2924 (1991).
- ¹¹M. Cardona, T. A. Meyer, and M. L. W. Thewalt, Phys. Rev. Lett. **92**, 196403 (2004).
- ¹²S. Hameau, Y. Guldner, O. Verzelen, R. Ferreira, G. Bastard, J. Zeman, A. Lemaitre, and J. M. Gérard, Phys. Rev. Lett. **83**, 4152 (1999).
- ¹³T. Inoshita and H. Sakaki, Phys. Rev. B **56**, R4355 (1997); O. Verzelen, R. Ferreira, and G. Bastard, Phys. Rev. Lett. **88**, 146803 (2002); M. I. Vasilevskiy, E. V. Anda, and S. S. Makler, Phys. Rev. B **70**, 035318 (2004).
- ¹⁴T. Vossmeier, L. Katsikas, M. Giersig, I. G. Popovic, K. Diesner, A. Chemseddine, A. Eychmüller, and H. Weller, J. Phys. Chem. **98**, 7665 (1994).
- ¹⁵A. Olkhovets, R.-C. Hsu, A. Lipovskii, and F. W. Wise, Phys. Rev. Lett. **81**, 3539 (1998).
- ¹⁶R. Pässler, Phys. Status Solidi B **236**, 710 (2003).
- ¹⁷R. Pässler, J. Appl. Phys. **89**, 6235 (2001).
- ¹⁸D. Bouwmeester, A. Ekert, and A. Zeilinger, *The Physics of Quantum Information* (Springer, Berlin, 2000).
- ¹⁹see, for example, A. Kiraz, P. Michler, C. Becher, B. Gayral, A. Imamoglu, L. Zhang, E. Hu, W. V. Schoenfeld, and P. M. Petroff, Appl. Phys. Lett. **78**, 3932 (2001).
- ²⁰Z. R. Wasilewski, S. Fafard, and J. P. McCaffrey, J. Cryst. Growth **201**, 1131 (1999).
- ²¹M. Galluppi, A. Frova, M. Capizzi, F. Boscherini, P. Frigeri, S. Franchi, and A. Passaseo, Appl. Phys. Lett. **78**, 3121 (2001).
- ²²I. Kegel, T. H. Metzger, A. Lorke, J. Peisl, J. Stangl, G. Bauer, J. M. Garcia, and P. M. Petroff, Phys. Rev. Lett. **85**, 1694 (2000).
- ²³D. M. Bruls, J. W. A. M. Vugs, P. M. Koenraad, H. W. M. Salemink, J. H. Wolter, M. Hopkinson, M. S. Skolnick, Fei Long, and S. P. A. Gill, Appl. Phys. Lett. **81**, 1708 (2002).
- ²⁴I. Favero, G. Cassabois, R. Ferreira, D. Darson, C. Voisin, J. Tignon, C. Delalande, G. Bastard, Ph. Roussignol, and J. M. Gérard, Phys. Rev. B **68**, 233301 (2003).
- ²⁵L. Besombes, K. Kheng, L. Marsal and H. Mariette, Phys. Rev. B **63**, 155307 (2001).
- ²⁶see, for example, J. Seufert, R. Weigand, G. Bacher, T. Kümmell, A. Forchel, K. Leonardi, and D. Hommel, Appl. Phys. Lett. **76**, 1872 (2000), and references therein.
- ²⁷J. H. Rice, J. W. Robinson, A. Jarjour, R. A. Taylor, R. A. Oliver, G. A. D. Briggs, M. J. Kappers, and C. J. Humphreys, Appl. Phys. Lett. **84**, 4110 (2004).
- ²⁸R. Seguin, S. Rodt, A. Strittmatter, L. Reissmann, T. Bartel, A. Hoffmann, D. Bimberg, E. Hahn, and D. Gerthsen, Appl. Phys. Lett. **84**, 4023 (2004).
- ²⁹E. Grilli, M. Guzzi, R. Zamboni, and L. Pavesi, Phys. Rev. B **45**, 1638 (1992).
- ³⁰Z. M. Fang, K. Y. Ma, D. H. Jaw, R. M. Cohen, and G. B. Stringfellow, J. Appl. Phys. **67**, 7034 (1990).
- ³¹See, for example, S. Fafard, S. Raymond, G. Wang, R. Leon, D. Leonard, S. Charbonneau, J. L. Merz, P. M. Petroff, and J. E. Bowers, Surf. Sci. **361/362**, 778 (1996); T. D. Happ, I. I. Tartakovskii, V. D. Kulakovskii, J.-P. Reithmaier, M. Kamp, and A. Forchel Phys. Rev. B **66**, 041303(R) (2002).
- ³²A. Vagov, V. M. Axt, and T. Kuhn, Phys. Rev. B **66**, 165312 (2002).
- ³³R. Pässler, J. Appl. Phys. **88**, 2570 (2000), and references therein.
- ³⁴R. Pässler, Phys. Status Solidi B **216**, 975 (1999), and references therein.
- ³⁵R. Pässler, Phys. Status Solidi B **200**, 155 (1997).
- ³⁶*Landolt-Börnstein: Numerical Data and Functional Relationships in Science and Technology*, edited by O. Madelung Vol. 17, Pt. A/B and Vol. 22, Pt. A (Springer, Berlin, 1989).
- ³⁷R. Pässler, Phys. Rev. B **66**, 085201 (2002).
- ³⁸R. Pässler, J. Appl. Phys. **90**, 3956 (2001).